

 Open access • Posted Content • DOI:10.1101/433623

## G-Protein signaling accelerates stem cell divisions in *Drosophila* males

— [Source link](#) 

Manashree Malpe, Leon F. McSwain, Karl Kudyba, Chun L. Ng ...+7 more authors

**Institutions:** University of Georgia, Emory University, University of Texas Southwestern Medical Center, University of North Georgia ...+1 more institutions

**Published on:** 02 Oct 2018 - bioRxiv (Cold Spring Harbor Laboratory)

**Topics:** Stem cell, Adult stem cell, Cellular differentiation and Germline

Related papers:

- [Twin Promotes the Maintenance and Differentiation of Germline Stem Cell Lineage through Modulation of Multiple Pathways](#)
- [Protein synthesis and degradation are essential to regulate germline stem cell homeostasis in \*Drosophila\* testes.](#)
- [Scratching the niche that controls \*Caenorhabditis elegans\* germline stem cells.](#)
- [Somatic Cell Encystment Promotes Abscission in Germline Stem Cells following a Regulated Block in Cytokinesis](#)
- [Jak-STAT regulation of male germline stem cell establishment during \*Drosophila\* embryogenesis.](#)

Share this paper:    

View more about this paper here: <https://typeset.io/papers/g-protein-signaling-accelerates-stem-cell-divisions-in-10mx834s4p>

1 **G-Protein signaling accelerates stem cell divisions in *Drosophila* males**

2 Manashree Malpe<sup>1,\*</sup>, Leon F. McSwain<sup>2,\*</sup>, Karl Kudyba<sup>1,\*</sup>, Chun L. Ng<sup>3</sup>, Jennie

3 Nicholson<sup>1</sup>, Maximilian Brady<sup>1</sup>, Yue Qian<sup>4</sup>, Vinay Choksi<sup>5</sup>, Alicia G. Hudson<sup>1</sup>, Benjamin

4 B. Parrott<sup>6</sup>, and Cordula Schulz<sup>1,#</sup>

5

6 1 Department of Cellular Biology, University of Georgia, Athens GA 30602, USA

7 2 Winship Cancer Institute, Emory University, Atlanta, GA 30322, USA

8 3 University of Texas Southwestern Medical Center, Dallas, TX

9 4 University of North Georgia, Department of Biology, Oakwood, GA 30566

10 5 School of Medicine, Duke University, Durham, NC 27708, USA

11 6 Odum School of Ecology, University of Georgia, Athens, GA 30602, USA

12 \* These authors contributed equally

13 # Corresponding author: cschulz@uga.edu

14

15

16

17

18

19

20

21

22

23

24 **Abstract**

25 Adult stem cells divide to renew the stem cell pool and replenish specialized cells that  
26 are lost due to death or usage. However, little is known about the mechanisms  
27 regulating how stem cells adjust to a demand for specialized cells. A failure of the stem  
28 cells to respond to this demand can have serious consequences, such as tissue loss, or  
29 prolonged recovery post injury.

30 Here, we challenge the male germline stem cells (GSCs) of *Drosophila*  
31 *melanogaster* for the production of specialized cells using mating experiments. We  
32 show that repeated mating reduced the sperm pool and accelerated germline stem cell  
33 (GSC) divisions. The increase in GSC divisions depended on the activity of the highly  
34 conserved G-proteins. Germline expression of RNA-Interference (RNA-*i*) constructs  
35 against G-proteins or a dominant negative G-protein eliminated the increase in GSC  
36 divisions in mated males. Consistent with a role for the G-proteins in the regulation of  
37 GSC divisions, RNA-*i* against seven out of 35 G-protein coupled receptors (GPCRs)  
38 within the germline cells also eliminated the capability of males to accelerate their GSC  
39 divisions in response to mating. Our data show that GSCs are receptive to GPCR  
40 stimulus, potentially through a network of interactions among multiple signaling  
41 pathways.

42

43 **Introduction**

44 Metazoan tissues undergo homeostasis wherein stem cells divide and their daughter  
45 cells proliferate and differentiate to replace lost cells. The human hematopoietic stem  
46 cells, for example, renew a remarkable number of about one trillion blood cells per day

47 <sup>1,2</sup>. Stem cells have to maintain a baseline mitotic activity for the production of daughter  
48 cells that account for the daily turnover of differentiated cells. However, whether stem  
49 cells can modulate their mitotic activity in response to demands that challenge the  
50 system is not fully explored. In some instances, stem cells respond to physiological  
51 cues; for example, murine hematopoietic stem cells divide more frequently during  
52 pregnancy due to increased oestrogen levels <sup>3</sup>. In *Drosophila melanogaster*, intestinal  
53 stem cells initiate extra cell divisions upon ablation of differentiated gut cells. *Drosophila*  
54 GSCs modulate their mitotic activity in response to environmental conditions, such as  
55 nutrient availability and temperature <sup>4-7</sup>.

56 *Drosophila* is an excellent model for identifying the molecules and mechanisms  
57 that regulate and fine-tune tissue homeostasis. A plethora of genetic tools are available  
58 for manipulating and monitoring dividing adult stem cells in *Drosophila*. The small size  
59 of the fly, the short generation cycle, and the fairly low costs covering their maintenance  
60 allow for high throughput screens. Here, we subjected several thousand male and  
61 several million virgin female flies to mating experiments, a task challenging to perform  
62 with vertebrate model organisms. We discovered that repeated mating caused a  
63 reproducible and significant increase in GSC division frequency in *Drosophila wild-type*  
64 (*wt*) males. Our analysis revealed that this response to mating was dependent on the  
65 activity G-proteins. Impairing G-protein activity from the germline cells eliminated the  
66 ability of the GSCs to increase their division frequency in response to mating.

67 G-proteins are highly conserved molecules that associate with GPCRs. GPCRs  
68 constitute a large family of cell surface receptors that mediate the cell's response to a  
69 wide range of external stimuli, including odors, pheromones, hormones, and

70 neurotransmitters. Loss of GPCR signaling affects countless developmental and neural  
71 processes in humans, as well as vertebrate and invertebrate model organisms<sup>8-10</sup>. Here  
72 we show that reducing the expression of seven out of 35 GPCRs via RNA-*i* from the  
73 germline cells eliminated the capability of males to accelerate their GSC divisions when  
74 mated. These were the Serotonin (5-HT) Receptors 1A, 1B and 7, Metuselah (Mth),  
75 Metuselah-like5 (Mth-l5), Octopamine $\beta$ 2-Receptor (Oct $\beta$ 2R), and a predicted GPCR  
76 encoded by *CG12290*.

77 A role for any of these GPCRs in regulating GSC division frequency is novel. No  
78 previous study has identified any functional role for Mth-l5 or CG12290. Serotonin,  
79 Octopamine, and Mth signaling play opposing roles in life-span, locomotion, and sleep  
80<sup>11-16</sup>. Mth signaling also regulates vesicle trafficking at the synapse, Octopamine  
81 signaling regulates ovulation, and Serotonin signaling plays essential roles in memory  
82 formation and learning<sup>17-19</sup>.

83

## 84 **Results**

### 85 **Mating increased the percentage of GSCs in mitosis**

86 As is typical for many stem cells, the *Drosophila* GSCs are found in a specific cellular  
87 microenvironment. They are located at the tip of the gonad, where they are attached to  
88 somatic hub cells (Figure 1A, A'). Upon GSC division, one of the daughter cells, called  
89 gonialblast, undergoes four rounds of stem cell daughter characteristic transit amplifying  
90 divisions, resulting in 16 spermatogonia. Subsequently, spermatogonia enter a tissue-  
91 specific differentiation process. They grow in size, undergo the two rounds of meiosis,  
92 and develop through extensive morphological changes into elongated spermatids<sup>20</sup>.

93 According to this tightly controlled homeostasis program, each GSC division can only  
94 produce 64 spermatids (Figure 1A). Thus, an increase in sperm production is reliant on  
95 the GSCs.

96 We investigate division frequency using an established immuno-fluorescence  
97 protocol <sup>7</sup>. In this approach, Vasa-positive GSCs are identified based on their position  
98 adjacent to FasciclinIII (FasIII)-positive hub cells (Figure 1A'). The percentage of GSCs  
99 in mitosis, the M-phase index (MI), is investigated by staining against phosphorylated  
100 Histone-H3 (pHH3). The MI of the GSCs ( $MI^{GSC}$ ) is calculated by dividing the number of  
101 pHH3-positive GSCs by the total number of GSCs.

102 To investigate if stem cells can modulate their division frequency in response to a  
103 demand for specialized cells, we challenged *Drosophila* males in mating experiments.  
104 For each experiment, 80-100 males were exposed individually to virgin females. An  
105 equal number of male siblings were each kept in solitude and served as the non-mated  
106 controls. To keep experimental variation to a minimum, we employed a three-day  
107 mating protocol for all experiments, kept the animals under the same conditions,  
108 dissected the testes at the same time of the same day, and dissected experimental  
109 groups in tandem. Using *wt* males, we obtained robust and reproducible increases in  
110  $MI^{GSC}$  in response to mating. The box-plot in Figure 1B shows the observed difference  
111 in  $MI^{GSC}$  between mated and non-mated populations of isogenized *wt*, *Oregon R (OR)*,  
112 males from 17 independent mating experiments. Interestingly, we observed variability in  
113  $MI^{GSC}$  among males of each condition. The  $MI^{GSC}$  of non-mated males ranged from six  
114 to nine percent, with a median at seven percent. The  $MI^{GSC}$  of mated males ranged from  
115 11 to 18 percent, with a median at 16.5 percent. We hypothesize that this variability in

116  $MI^{GSC}$  within each condition is due to naturally occurring physiological differences within  
117 the flies. Likewise, the increase in  $MI^{GSC}$  in response to mating varied among the  
118 different experiments, but, in each of the experiments, the increase was biologically and  
119 statistically significant.

120 We next investigated if only a few males within a population contributed to the  
121 increase in  $MI^{GSC}$  or whether the effect of mating is reflected by changes in the  $MI^{GSC}$   
122 across a population. These data are displayed in frequency distribution graphs (FDGs).  
123 FDGs show how often a particular value is represented within a population. When the  
124 distribution of the  $MI^{GSC}$  for testes within one population of *OR* flies was plotted, the  
125 resulting FDG revealed that mated males had significantly fewer testes with an  $MI^{GSC}$  of  
126 zero and more testes with higher  $MI^{GSC}$  compared to non-mated siblings (Figure 1C).  
127 We observed the same result for another isogenized *wt* strain, *Canton S* (*CS*, Figure  
128 1D). We conclude that mating affected the  $MI^{GSC}$  of many males within one mated  
129 population.

130 Finally, we asked how long or frequently we had to mate the males to see an  
131 increase in  $MI^{GSC}$ . For this, we mated *OR* males to varying numbers of virgin females  
132 and subsequently analyzed how many of their GSCs were in mitotic division. When we  
133 exposed *OR* males for 24 hours to one (1F, 24 hrs), two (2F, 24 hrs), or three (3F,  
134 24hrs) female virgins, no significant difference in  $MI^{GSC}$  between non-mated and mated  
135 males was apparent (Figure S1A). Robust and reproducible increases were seen in *OR*  
136 males that were exposed to three virgin females on each of two (2x3F, 48 hrs) or three  
137 (3x3F, 72 hrs) days of mating (Figure S1A). We conclude that males have to mate  
138 repeatedly for an increase in  $MI^{GSC}$  to occur. The increase in  $MI^{GSC}$  in mated males was

139 reversible, showing that the response to mating was dynamic. Moving males back into  
140 solitude after the three-day mating experiment for 48 hours (3x3F, 120 hrs) eliminated  
141 the increase in  $MI^{GSC}$  (Figure S1A). Control males mated for 120 hours (5x3F, 120 hrs),  
142 in contrast, still had a significant increase in  $MI^{GSC}$  (Figure S1A).

143

#### 144 **Mating increased GSC division frequency**

145 As another measure of cell divisions, we investigated the percentage of GSCs in  
146 synthesis phase (S-phase) of the cell cycle. Testes were labeled with 5-ethynyl-2'-  
147 deoxyuridine (EdU) and the S-phase index of the GSCs ( $SI^{GSC}$ ) was calculated by  
148 dividing the number of EdU-positive GSCs by the total number of GSCs. Using pulse-  
149 labeling experiments, we observed that mated *OR* males displayed significant higher  
150  $SI^{GSC}$  compared to their non-mated siblings (Figure 1E). Together with the increase in  
151 the  $MI^{GSC}$  this suggests that mating accelerates stem cell divisions.

152 To test this hypothesis, the lengths of the cell cycle were measured using EdU  
153 feeding experiments. In this approach, *OR* animals were fed EdU during the mating  
154 experiment. We then calculated how many GSCs had been in S-phase at different time  
155 points. Our EdU-incorporation experiment revealed that the number of EdU-positive  
156 GSCs increased rapidly after 24 hours of feeding and reached 80% at 60 hours of  
157 feeding (Figure 1F). Prolonged feeding further increased the numbers of EdU-positive  
158 GSCs but this data was excluded from the study as the majority of males that were fed  
159 EdU while mating had died by 72 hours of the experiment. The response curve we  
160 obtained in this time-course experiment is different from the response curves reported  
161 by other groups that used bromo-deoxy-uridine (BrDU) as the thymidine analog instead



162 of EdU. For example, the non-mated males in our experiment had about 70% of EdU-  
163 positive GSCs after 48 hours of feeding. A study using *white (w)* mutant animals fed the  
164 same concentration of the thymidine homologue had a steeper response curve, in which  
165 85% of the GSCs were BrDU-marked after 48 hours of feeding <sup>21</sup>. Another study using  
166 *yellow, vermilion (y, v)* flies showed even steeper response curves where 100% of the  
167 GSCs were BrDU-labeled after 24 hours. However, in this study, animals were fed a 30  
168 times higher concentration of the thymidine homologue than used in our study <sup>22</sup>. We  
169 propose that the different response curves are due to the different genetic backgrounds,  
170 chemicals and doses.

171 Most importantly, mated males had significantly more EdU-positive GSCs at 36  
172 and 48 hours of mating compared to their non-mated siblings (Figure 1F). This  
173 experiment shows that, in mated males, more GSCs had entered S-phase of the cell  
174 cycle. We conclude that mated males had accelerated GSC divisions.

175 To further investigate how mating affects the cell cycle, we employed the Fly-  
176 Fucci technology in combination with the UAS-Ga4 expression system (Duffy, 2002  
177 #321)(Phelps, 1998 #34)(Zielke, 2014 #1122). With Fly-Fucci, the coding regions of  
178 fluorescent proteins are fused to the destruction boxes of cell cycle regulators, allowing  
179 the marking of different cell cycle stages. These artificial proteins are expressed under  
180 control of the Yeast Upstream Activating Sequences <sup>23</sup> (Zielke, 2014 #1122). UAS-  
181 controlled target genes can be expressed under spatial control using tissue-specific  
182 Gal4-transactivators. In addition, temporal control can be applied to their expression by  
183 exposing the flies to different temperatures (Phelps, 1998 #34)(Duffy, 2002 #321). For  
184 our experiments, we used a *nanos-Gal4*-transactivator (NG4) with a reported

185 expression in GSCs, gonialblasts, and spermatogonia (Van Doren, 1998 #55). Using  
186 two independent Fucci-lines, we observed that  $MI^{GSC}$  did not significantly increase in  
187 mated *Fucci/NG4* males while mated controls animals (*Fucci/wt*) increased their  $MI^{GSC}$   
188 compared to non-mated siblings (Figure S1B). We conclude that expressing FUCCI-  
189 constructs from these fly lines within the GSCs interfered with their ability to significantly  
190 increase  $MI^{GSC}$  in response to mating. One possible explanation for this could be that  
191 the expression of proteins with destruction boxes could overload the cell cycle  
192 machinery of male GSCs.

193

#### 194 **Mating reduced the sperm pool**

195 To confirm that our mating experiments created a demand for sperm, we explored  
196 differences in the sperm pool of the seminal vesicles between non-mated and mated  
197 males. For this, we used two different transgenic constructs that label the sperm. A Don  
198 Juan-Green Fluorescent Protein (DJ-GFP) reporter labels the sperm bodies and allows  
199 to assess the overall amount of sperm within the seminal vesicles<sup>24</sup>. A ProtamineB-  
200 GFP (Mst35B-GFP) line, on the other hand, only labels the sperm heads and can be  
201 used to count the sperm within the seminal vesicles<sup>25</sup>. With each of these reporters,  
202 individualized mature sperm was normally seen within the seminal vesicle of the male  
203 reproductive tract.

204 According to the literature, the total number of sperm within one seminal vesicle  
205 varies among different *Drosophila* species and among genetic backgrounds<sup>25-27</sup>. To  
206 keep the genetic background consistent among our experiments, we crossed each of  
207 the reporter lines to *OR* females and used their male progeny for our mating

208 experiments. The seminal vesicles were then analyzed at days one to three of the  
209 experiment. Based on the size and the fluorescence of the seminal vesicles, we first  
210 sorted them into three classes. Class 1 and class 2 seminal vesicles were completely  
211 filled with GFP-positive sperm heads. However, class 1 seminal vesicles were very wide  
212 (Figure 2A), while class 2 seminal vesicles were thinner (Figure 2B). Class 3 seminal  
213 vesicles contained only few GFP-positive sperm heads and had areas that were not  
214 filled with GFP (Figure 2C, arrows). A quantification revealed that non-mated males had  
215 mostly class 1 and 2 seminal vesicles, while mated males had mostly class 3 seminal  
216 vesicles. While we still detected class 1 and 2 seminal vesicles in males that had mated  
217 for only one day, their numbers were severely reduced in males after two and three  
218 days of mating (Figure 2D-F).

219 To further validate our observation that mating reduces the amount of sperm, we  
220 developed an automated procedure that calculates the volume occupied by Mst35B-  
221 GFP-positive sperm heads per seminal vesicle in all focal planes (voxels in Figure 2G).  
222 This allowed us to investigate larger numbers of seminal vesicles compared to a  
223 previously reported method, in which images through the seminal vesicles were  
224 flattened and sperm heads counted by eye<sup>25</sup>. Furthermore, a computer-based  
225 calculation eliminates subjective bias introduced by the investigator. Based on our  
226 computer calculation, the sperm heads of mated males occupied significantly less  
227 volume within the seminal vesicles than the sperm in non-mated males (Figure 2G).  
228 Notably, the total volume occupied by sperm became more reduced with every day of  
229 mating. By days two and three of mating it ranged from 0.1 to 0.4 x 10<sup>6</sup> voxels per  
230 seminal vesicle. The non-mated sibling controls, in contrast, maintained a large GFP-

231 occupied volume in their seminal vesicles, with an average of  $1.2 \times 10^6$  voxels per  
232 seminal vesicle. The computer program estimated the numbers of sperm per seminal  
233 vesicle of non-mated males around 2000, while males that were mated for two or three  
234 days had less than 500 sperm in their seminal vesicles. As our mated males showed a  
235 drastic reduction in sperm, we argue that we have created a demand for sperm.

236

### 237 ***Mating had no effect on GSC numbers***

238 It was previously reported that females significantly increased the numbers of their  
239 GSCs upon mating<sup>28</sup>. According to the literature, an adult male gonad contains up to  
240 twelve GSCs per testis, but the exact number of GSCs per testes appears to vary  
241 among different strains and laboratories. One study using a *wt* strain of males reported  
242 six to ten GSCs per testis, while other studies using transgenic males in a *w* mutant  
243 genetic background reported 8.94 and 12.3 GSCs per testis, respectively<sup>29-31</sup>. Among  
244 our fly lines, we found variation in GSC numbers as well. The distribution of GSCs  
245 ranged from one to 14 per testis, with an average of seven GSCs per testis. Males from  
246 an isogenized *OR* stock had the lowest average number of GSCs, having only four to  
247 five GSCs per testis (Figure 3A). Males from an isogenized *CS* stock had an average of  
248 six GSCs per testis (Figure 3B). Animals mutant for *w* alleles, *w*<sup>1118</sup> and *w*<sup>1</sup>, had on  
249 average eight and seven GSCs per testis, respectively (Figures 3C, 3D). Males from a  
250 *v*<sup>1</sup>, *y*<sup>1</sup> stock, which serves as the genetic background for many RNA-*i* lines, had the  
251 highest average number of GSCs, at 11 GSCs per testis (Figure 3E). We believe that  
252 the obtained GSC numbers are specific to the fly lines in our laboratory and do not  
253 necessarily reflect the numbers of GSCs in fly stocks of other laboratories.

254           Importantly, we did not observe a significant difference in the numbers of GSCs  
255 between non-mated and mated siblings in any of these fly lines (Figure 3A-E). We  
256 concluded that mating did not affect the numbers of GSCs in our fly stocks. However,  
257 the observed variation in GSC numbers prompted us to perform our experiments in  
258 animals from as similar genetic backgrounds as possible. All males reported in the  
259 following of this manuscript carried the X-chromosome from our isogenized *OR* line.

260

### 261 ***The increase in $MI^{GSC}$ upon mating required G-protein signaling***

262 *Drosophila* mating is a complex and genetically controlled behavior that is dependent on  
263 neural circuits<sup>32</sup>. This implicates a possible neuronal control in regulating GSC divisions  
264 during mating. Therefore, we wanted to focus on the type of signaling pathway  
265 commonly stimulated during neural activity, G-protein signaling<sup>33, 34</sup>. In a non-stimulated  
266 cell, a trimeric complex of G-proteins,  $G_{\alpha}$ ,  $G_{\beta}$ , and  $G_{\gamma}$  is associated with classical  
267 GPCRs (Figure 4A, step 1). When ligand binds to the GPCR, a guanidyl exchange  
268 factor within the GPCR becomes activated that exchanges GDP for GTP in the  $G_{\alpha}$   
269 subunit. The exchange leads to the dissociation of  $G_{\alpha}$  and the  $G_{\beta/\gamma}$  complex from each  
270 other and from the GPCR. Remaining attached to the membrane,  $G_{\alpha}$  and  $G_{\beta/\gamma}$  diffuse  
271 along it and activate downstream signal transducers (Figure 4A, step 2)<sup>35, 36</sup>. Most  
272 organisms have multiple genes that encode for each of the G-protein subunits.  
273 *Drosophila* has six  $G_{\alpha}$ , three  $G_{\beta}$ , and two  $G_{\gamma}$  proteins, yet only a few examples are  
274 available in the literature associating a specific *Drosophila* G-protein with an upstream  
275 GPCR<sup>35, 37</sup>.

276           Animals mutant for G-protein subunits are often lethal, making it problematic to  
277 investigate their roles in the adult. Furthermore, studying G-protein signaling in animals  
278 lacking their function throughout the whole body may could affect behavior and  
279 physiology of the fly, leading to confounding effects on mating and GSC divisions.  
280 Fortunately, large collections of RNA-*i*-lines are available that are expressed under  
281 control of UAS. To reduce G-protein signaling we employed two separate *nanos*-Gal4-  
282 transactivators (*NG4*), *NG4-1* and *NG4-2*. When RNA-*i* against the different G-protein  
283 subunit was expressed within the germline cells via *NG4-1*, several of the mated males  
284 displayed only a weak increase in MI<sup>GSC</sup> compared to their non-mated siblings (Table  
285 1). We focused on an RNA-*i*-line that is directed against the subunit *G $\alpha$ i* as animals  
286 expressing this construct within the germline did not show any increase in MI<sup>GSC</sup> in  
287 response to mating (Table 1). For reproducibility, we conducted each of the following  
288 experiments in triplicates. We used progeny from transgenic Gal4 and UAS-flies that  
289 had been crossed to *wt* as positive controls. As expected, each population of positive  
290 control males displayed a significant increase in MI<sup>GSC</sup> when mated (Figure 4B).  
291 Experimental flies expressing *G $\alpha$ i-i* via *NG4-1* or *NG4-2*, however, failed to increase  
292 MI<sup>GSC</sup> (Figure 4C).

293           We next sought to validate the role for G-protein signaling in GSC division  
294 frequency by an alternative approach. A dominant negative version of *Drosophila* G $\gamma$ 1  
295 (dnG $\gamma$ 1) is available that serves as a reliable tool to abolish G-protein signaling<sup>38</sup>. Males  
296 expressing dnG $\gamma$ 1 via either *NG4-1* or *NG4-2* did not show an increase in MI<sup>GSC</sup> in  
297 response to mating (Figure 3C). Control dnG $\gamma$ 1/*wt* animals, on the other hand, had  
298 increased MI<sup>GSC</sup> upon mating (Figure 3B). These data clearly show that signaling via G-

299 proteins is required for the increase in MI<sup>GSC</sup>. Plotting the results in FDGs confirmed that  
300 mated control animals had significantly fewer testes with an MI<sup>GSC</sup> of zero and more  
301 testes with higher MI<sup>GSC</sup> compared to non-mated males (Figures S3A-D), and that this  
302 response to mating was eliminated in experimental males (Figures S3E-H).

303 In mammalian cells, three major G-protein-dependent signaling cascades have  
304 been described (Figure 3A, steps 3a, b, c)<sup>33, 39</sup>. For *Drosophila*, the literature provides  
305 little information on the signaling cascades downstream of GPCRs but it is generally  
306 assumed that the mammalian signal transducers are conserved in flies. To further  
307 validate that an increase in MI<sup>GSC</sup> upon mating is regulated by G-protein signaling we  
308 expressed RNA-*i* and mis-expression constructs for conserved signal transducers via  
309 NG4 and found that males expressing RNA-*i*-lines for one of the *Drosophila Protein*  
310 *Kinase C (PKC)* proteins, *PKC98E*, for *Inositol-triphosphate 3-Kinase (IP3K)*, and for  
311 *Ca<sup>2+</sup>/Calmodulin-dependent protein kinase II (CaMKII)* indeed failed to increase MI<sup>GSC</sup>  
312 in response to mating (Table 1).

313

### 314 ***RNA-i against seven distinct GPCRs blocked the increase in MI<sup>GSC</sup> upon mating***

315 To further confirm that G-protein signaling regulates the increase in MI<sup>GSC</sup> we aimed  
316 towards identifying the upstream GPCRs. Next Generation Sequencing (NGS) of RNA  
317 from *wt* testis tips revealed the expression of 140 receptors, including 35 classical  
318 GPCRs (Figure 5 and Table 2). The functions of many of these GPCRs have not been  
319 studied yet and mutant animals are only available in rare cases. Expressing RNA-*i*-  
320 constructs against most GPCRs in the germline had little to no effect on the ability of the  
321 GSCs to increase their MI<sup>GSC</sup> in response to mating (Table 2). RNA-*i* against three

322 Serotonin Receptors (5HT-1A, 5HT-1B and 5HT-7), Mth, Mth-I5, Oct $\beta$ 2R, and a  
323 predicted GPCR encoded by CG12290, clearly and reproducibly eliminated this ability.  
324 Animals carrying UAS-controlled RNA-*i*-constructs against these GPCRs (*GPCR-i*) were  
325 crossed to *wt*, *NG4-1* and *NG4-2*, and MI<sup>GSC</sup> of their progeny was investigated. Each of  
326 the controls (*GPCR-i/wt*) increased their MI<sup>GSC</sup> when repeatedly mated to females in  
327 each of the triplicate experiments (Figure 5A and Figures S3A-G). However, when the  
328 *GPCR-i*-animals were crossed with either *NG4-1* (Figure 5B and Figures S3H-N) or  
329 *NG4-2* (Figure 5C and Figures S3O-U) the MI<sup>GSC</sup> of their non-mated and mated progeny  
330 did not significantly differ. Confirming the necessity of the GPCRs in increasing MI<sup>GSC</sup>,  
331 we investigated alternative RNA-*i*-lines. A second RNA-*i*-line for Mth blocked the  
332 increase in MI<sup>GSC</sup> in mated males and a second RNA-*i*-line for 5HT-1A displayed only a  
333 weak response to mating (Table 3).

334 Mating success was evaluated by two criteria: visual observation and the  
335 appearance of progeny. When flies were anesthetized to exchange the females for  
336 fresh virgins, several copulating pairs of males and females were always observed.  
337 Furthermore, 100 single females that had been exposed to males on day one of the  
338 experiment were placed into one food vial each and mating success evaluated a few  
339 days later by counting the percentage of vials with progeny. Most males in this study  
340 sired 60-90% of the females. Specifically, each of the *GPCR-i/NG4-1* males produced  
341 offspring (Table S1), showing that a block in the increase in MI<sup>GSC</sup> is not caused by a  
342 failure to mate but by a lack of GPCR signaling. Viable alleles of 5HT-1A and 5HT-1B  
343 were not pursued as alternative strategies because they displayed only a weak mating  
344 success rate (Table S1).



345           Finally, we wanted to assure that male age had no effect on the increase in  
346  $MI^{GSC}$ . We performed a time-course experiment of one, two, three, and four-week old  
347 *OR* males. We found that mated males of all ages showed robust increases in  $MI^{GSC}$   
348 compared to their non-mated siblings (Figure S1C). We conclude that aging animals for  
349 up to four weeks had little to no effect on the ability of *wt* GSCs to increase their  $MI^{GSC}$   
350 in response to mating, and that the age of the transgenic animals used in this study  
351 (three weeks of age at the time of testes dissection) had no impact on the obtained  
352 results.

353

## 354 **Discussion**

355           Here, we show that repeated mating reduced the sperm pool and increased GSC  
356 division frequency. Using highly controlled experiments, we demonstrate that mated  
357 males had more GSCs in M-phase and S-phase of the cell cycle compared to non-  
358 mated males. Mated males also showed faster incorporation of EdU indicating that their  
359 GSCs progressed faster through the cell cycle. Our findings demonstrate that GSCs can  
360 respond to a demand for sperm by accelerating their mitotic activity. Based on *RNA-i*  
361 targeting G-proteins and a dominant negative construct against  $G_{\gamma}1$ , the increase in  
362  $MI^{GSC}$  of mated males is dependent on G-protein signaling. Furthermore, signal  
363 transducers predicted to act downstream of G-proteins and GPCRs predicted to act  
364 upstream of G-proteins also appeared to be required for the response to mating.

365           Due to the lack of mutants and a potential interference of whole animal knock-  
366 down in the behavior of the flies, we used tissue-specific expression of *RNA-i*-  
367 constructs. It is surprising that our studies revealed potential roles for seven instead of a

368 single GPCR in the increase of MI<sup>GSC</sup> in response to mating. A possible explanation is  
369 that some of the RNA-*i*-lines have off-target effects. RNA-*i*-hairpins can cause the  
370 down-regulation of unintended targets due to stretches of sequence homologies,  
371 especially when long hairpins are used<sup>40, 41</sup>. However, with the exception of the RNA-*i*-  
372 line directed against 5HT-7, all lines that produced a phenotype contain second  
373 generation vectors with a short, 21 nucleotide hairpin predicted to have no off-target  
374 effects<sup>42</sup>. We hypothesize that multiple GPCRs regulate the increase in MI<sup>GSC</sup> in  
375 response to mating. Consistent with this, expression of second RNA-*i*-line directed  
376 against Mth or 5HT-1A interfered with the increase in MI<sup>GSC</sup> in mated males.

377 Our finding that RNA-*i* against several GPCRs blocked the increase in MI<sup>GSC</sup> in  
378 mated males suggests a high level of complexity in the regulation of GSC divisions. In  
379 the literature, increasing evidence has emerged that GPCRs can form dimers and  
380 oligomers and that these physical associations have a variety of functional roles,  
381 ranging from GPCR trafficking to modification of G-protein mediated signaling<sup>43-45</sup>. In *C.*  
382 *elegans*, two Octopamine receptors, SER-3 and SER-6, additively regulate the same  
383 signal transducers for food-deprived-mediated signaling. One possible explanation for  
384 the non-redundant function of the two receptors was the idea that they form a functional  
385 dimer<sup>46</sup>. In mammalian cells, 5-HT receptors can form homo-dimers and hetero-dimers  
386 and, dependent on this, have different effects on G-protein signaling<sup>47-49</sup>. In cultured  
387 fibroblast cells, for example, G-protein coupling is more efficient when both receptors  
388 within a 5-HT4 homo-dimer bind to agonist instead of only one<sup>50</sup>. In cultured  
389 hippocampal neurons, hetero-dimerization of 5-HT1A with 5-HT7 reduces G-protein  
390 activation and decreases the opening of a potassium channel compared to 5-HT1A

391 homo-dimers<sup>51</sup>. The formation of hetero-dimers of GPCRs with other types of receptors  
392 plays a role in depression and in the response to hallucinogens in rodents<sup>52, 53</sup>.

393         Alternatively, or in addition to the possibility that some or all of the seven GPCRs  
394 form physical complexes, a role for several distinct GPCRs in regulating GSC division  
395 frequency could be explained by crosstalk among the downstream signaling cascades.  
396 One signaling cascade could, for example, lead to the expression of a kinase that is  
397 activated by another cascade. Similarly, one signaling cascade could open an ion  
398 channel necessary for the activity of a protein within another cascade. Unfortunately,  
399 the literature provides little information on *Drosophila* GPCR signal transduction  
400 cascades and only very few mutants have been identified that affect a process  
401 downstream of GPCR stimulation. Thus, it remains to be explored how stimulation of  
402 the GPCRs and G-proteins increase GSC divisions.

403         The role for G-protein signaling in regulating the frequency of stem cell divisions  
404 is novel. Our data suggest that the increase in MI<sup>GSC</sup> in response to mating is regulated  
405 by external signals, potentially arising from the nervous system, that stimulate G-protein  
406 signaling within the GSCs. Based on the nature of the GPCRs, the activating signal  
407 could be Serotonin, the Mth ligand, Stunted, Octopamine, or two other, yet unknown,  
408 signals that activate Mth-I5, and CG12290<sup>54-56</sup>. It will be interesting to address which of  
409 these ligands are sufficient to increase MI<sup>GSC</sup>, in what concentrations they act, by which  
410 tissues they are released, and whether they also affect other stem cell populations.

411

## 412 **Methods**

### 413 ***Fly husbandry***

414 Flies were raised on a standard cornmeal/agar diet and maintained in temperature-,  
415 light-, and humidity-controlled incubators. Unless otherwise noted, all mutations,  
416 markers, and transgenic lines are described in the *Drosophila* database and were  
417 obtained from the Bloomington stock center (Consortium, 2003 #132).

418

### 419 ***UAS/Gal4-expression studies***

420 Two separate X; UAS-*dicer*; nanos-*Gal4* (NG4-1 and NG4-2) fly lines were used as  
421 transactivators. Females from the transactivator line or *wt* females were crossed with  
422 males carrying target genes under the control of UAS in egg lay containers with fresh  
423 apple juice-agar and yeast paste to generate either experimental or control flies. The  
424 progeny were transferred into food bottles, raised to adulthood at 18°C, males collected  
425 and then shifted to 29°C for seven days to induce high activity of Gal4 prior to the  
426 mating experiment. Note that the males were not collected as virgins as to avoid any  
427 potential developmental or learning effects on our experiments.

428

### 429 ***Mating experiments***

430 Unless otherwise noted, mating experiments were performed at 29°C. Males and virgin  
431 females were placed on separate apple juice-agar plates with yeast paste overnight to  
432 assure they were well fed prior to their transfer into mating chambers. Single males  
433 were placed into each mating slot either by themselves (non-mated) or with three virgin  
434 females (mated) and the chambers closed with apple juice-agar lids with yeast paste.  
435 Females were replaced by virgin females on each of the following two days and apple  
436 juice-agar lids with yeast paste were replaced on a daily basis for both non-mated and

437 mated animals. In most instances, females from the stock  $X^{\square}X, y, w, f / Y / shi^{ts}$  were  
438 used as virgins. When raised at 29°C, only females hatch from this stock. For fertility  
439 tests, *OR* virgins were used. Note that 10-20% of the mated males died during the  
440 experiment while only 5% of the non-mated siblings died.

441

#### 442 ***Immuno-fluorescence and microscopy***

443 Animals were placed on ice to immobilize them. Gonads were dissected in Tissue  
444 Isolation Buffer (TIB) and collected in a 1.5 ml tube with TIB buffer on ice for no more  
445 than 30 minutes. Gonads were then fixed, followed by immuno-fluorescence staining  
446 and imaging as previously described <sup>7</sup>. The mouse anti-FasciclinIII (FasIII) antibody  
447 (1:10) developed by C. Goodman was obtained from the Developmental Studies  
448 Hybridoma Bank, created by the NICHD of the NIH and maintained at The University of  
449 Iowa, Department of Biology, Iowa City, IA 52242. Goat anti-Vasa antibody (1:50 to  
450 1:300) was obtained from Santa Cruz Biotechnology Inc. (sc26877), anti-  
451 phosphorylated Histone H3 (pHH3) antibodies (1:100 to 1:1000) were obtained from  
452 Fisher (PA5-17869), Millipore (06-570), and Santa Cruz Biotechnology Inc. (sc8656-R).  
453 Secondary Alexa 488, 568, and 647-coupled antibodies (1:1000) and Slow Fade Gold  
454 embedding medium with DAPI were obtained from Life Technologies. Images were  
455 taken with a Zeiss Axiophot, equipped with a digital camera, an apotome, and  
456 Axiovision Rel. software. Statistical relevance was determined using the two-tailed  
457 Graphpad student's t-test.

458

#### 459 ***EdU-labeling experiments***

460 The EdU-labeling kit was obtained from Invitrogen and the procedure performed  
461 following manufacturer's instructions. For EdU-pulse labeling experiments, animals  
462 were mated as described above, and the dissected testes incubated with 10mM EdU in  
463 PBS for 30 minutes at room temperature prior to fixation. For EdU-feeding experiments,  
464 *OR* males were fed 10 mM EdU in liquid yeast provided on paper towels. These animals  
465 were mated at room temperature (21°C) because the paper towels easily dried out at  
466 higher temperatures, causing the flies to dehydrate and die.

467

#### 468 ***Sperm head volumetric calculations***

469 In order to easily evaluate sperm numbers, we turned to computer analysis in Python.  
470 By quantifying the volume of GFP signal we generated estimates to the amount of  
471 sperm in each seminal vesicle. Image stacks were taken of individual seminal vesicles.  
472 After masking relevant regions, each image set was normalized by mean subtraction  
473 and division by the standard deviation, followed by rescaling image intensity to  
474 encompass the range of the image. To remove signal noise, a median filter was applied  
475 and the mask refined by Otsu thresholding. We determined signal volume by hysteresis  
476 thresholding. This approach initially thresholds an image at an upper limit, and then  
477 expands the region by adjacent pixels satisfying the lower threshold. We set the lower  
478 bound at the value generated from a triangle threshold and the upper threshold as the  
479 median value above the lower limit. The number of signal voxels was calculated and  
480 normalized to an expected size of a single sperm head. Our analysis utilized OpenCV  
481 3.4.2, Scipy1.2.1, Scikit-image 0.14.2, Numpy 1.16.2, Matplotlib 3.0.3, Seaborn 0.9.0,  
482 as well as built in Python 3.7.3 modules<sup>57-61</sup>.

483

484 **References**

485

- 486 1. Dancey, J.T., Deubelbeiss, K.A., Harker, L.A. & Finch, C.A. Neutrophil kinetics in  
487 man. *J Clin Invest* **58**, 705-715 (1976).
- 488 2. Erslev, A. Production of erythrocytes, in *Hematology*. (ed. B.E. William WJ,  
489 Erslev AJ, Lichtman MA) 365-376 (  
490 Mc-Graw-Hill, New York, NY; 1983).
- 491 3. Nakada, D. *et al.* Oestrogen increases haematopoietic stem-cell self-renewal in  
492 females and during pregnancy. *Nature* **505**, 555-558 (2014).
- 493 4. Hsu, H.J., LaFever, L. & Drummond-Barbosa, D. Diet controls normal and  
494 tumorous germline stem cells via insulin-dependent and -independent  
495 mechanisms in *Drosophila*. *Dev Biol* **313**, 700-712 (2008).
- 496 5. Amcheslavsky, A., Jiang, J. & Ip, Y.T. Tissue damage-induced intestinal stem  
497 cell division in *Drosophila*. *Cell Stem Cell* **4**, 49-61 (2009).
- 498 6. McLeod, C.J., Wang, L., Wong, C. & Jones, D.L. Stem cell dynamics in response  
499 to nutrient availability. *Curr Biol* **20**, 2100-2105 (2010).
- 500 7. Parrott, B.B., Hudson, A., Brady, R. & Schulz, C. Control of germline stem cell  
501 division frequency--a novel, developmentally regulated role for epidermal growth  
502 factor signaling. *PLoS One* **7**, e36460 (2012).
- 503 8. Schoneberg, T. *et al.* Mutant G-protein-coupled receptors as a cause of human  
504 diseases. *Pharmacol Ther* **104**, 173-206 (2004).

- 505 9. Wettschureck, N. & Offermanns, S. Mammalian G proteins and their cell type  
506 specific functions. *Physiol Rev* **85**, 1159-1204 (2005).
- 507 10. Langenhan, T. *et al.* Model Organisms in G Protein-Coupled Receptor Research.  
508 *Mol Pharmacol* **88**, 596-603 (2015).
- 509 11. Lin, Y.J., Seroude, L. & Benzer, S. Extended life-span and stress resistance in  
510 the *Drosophila* mutant methuselah. *Science* **282**, 943-946 (1998).
- 511 12. Selcho, M., Pauls, D., El Jundi, B., Stocker, R.F. & Thum, A.S. The role of  
512 octopamine and tyramine in *Drosophila* larval locomotion. *J Comp Neurol* **520**,  
513 3764-3785 (2012).
- 514 13. Silva, B., Goles, N.I., Varas, R. & Campusano, J.M. Serotonin receptors  
515 expressed in *Drosophila* mushroom bodies differentially modulate larval  
516 locomotion. *PLoS One* **9**, e89641 (2014).
- 517 14. Crocker, A. & Sehgal, A. Octopamine regulates sleep in *Drosophila* through  
518 protein kinase A-dependent mechanisms. *J Neurosci* **28**, 9377-9385 (2008).
- 519 15. Yuan, Q., Joiner, W.J. & Sehgal, A. A sleep-promoting role for the *Drosophila*  
520 serotonin receptor 1A. *Curr Biol* **16**, 1051-1062 (2006).
- 521 16. Li, Y. *et al.* Octopamine controls starvation resistance, life span and metabolic  
522 traits in *Drosophila*. *Sci Rep* **6**, 35359 (2016).
- 523 17. Song, W. *et al.* Presynaptic regulation of neurotransmission in *Drosophila* by the  
524 g protein-coupled receptor methuselah. *Neuron* **36**, 105-119 (2002).
- 525 18. Lee, H.G., Seong, C.S., Kim, Y.C., Davis, R.L. & Han, K.A. Octopamine receptor  
526 OAMB is required for ovulation in *Drosophila melanogaster*. *Dev Biol* **264**, 179-  
527 190 (2003).



- 528 19. Sitaraman, D. *et al.* Serotonin is necessary for place memory in *Drosophila*. *Proc*  
529 *Natl Acad Sci U S A* **105**, 5579-5584 (2008).
- 530 20. Fuller, M.T. Spermatogenesis, in *The development of Drosophila melanogaster*,  
531 Vol. 1. (ed. M. Bate, Martinez-Arias, A) 71-147 (Cold Spring Harbor Press, Cold  
532 Spring Harbor; 1993).
- 533 21. Wallenfang, M.R., Nayak, R. & DiNardo, S. Dynamics of the male germline stem  
534 cell population during aging of *Drosophila melanogaster*. *Aging Cell* **5**, 297-304  
535 (2006).
- 536 22. Yang, H. & Yamashita, Y.M. The regulated elimination of transit-amplifying cells  
537 preserves tissue homeostasis during protein starvation in *Drosophila* testis.  
538 *Development* **142**, 1756-1766 (2015).
- 539 23. Abdouh, M., Albert, P.R., Drobetsky, E., Filep, J.G. & Kouassi, E. 5-HT1A-  
540 mediated promotion of mitogen-activated T and B cell survival and proliferation is  
541 associated with increased translocation of NF-kappaB to the nucleus. *Brain*  
542 *Behav Immun* **18**, 24-34 (2004).
- 543 24. Santel, A., Blumer, N., Kampfer, M. & Renkawitz-Pohl, R. Flagellar mitochondrial  
544 association of the male-specific Don Juan protein in *Drosophila* spermatozoa. *J*  
545 *Cell Sci* **111 ( Pt 22)**, 3299-3309 (1998).
- 546 25. Tirmarche, S. *et al.* *Drosophila* protamine-like Mst35Ba and Mst35Bb are  
547 required for proper sperm nuclear morphology but are dispensable for male  
548 fertility. *G3 (Bethesda)* **4**, 2241-2245 (2014).
- 549 26. Pitnick, S., Markow, T.A. Male gametic Strategies: Sperm Size, Testes Size, and  
550 the Allocation of Ejaculate among Successive Mates by the Sperm-Limited Fly

- 551           Drosophila Pachea and its Relatives. *The American Naturalist* **143**, 785-819  
552           (1994).
- 553 27.       Kubrak, O.I., Kucerova, L., Theopold, U., Nylin, S. & Nassel, D.R.  
554           Characterization of Reproductive Dormancy in Male *Drosophila melanogaster*.  
555           *Front Physiol* **7**, 572 (2016).
- 556 28.       Ameku, T. & Niwa, R. Mating-Induced Increase in Germline Stem Cells via the  
557           Neuroendocrine System in Female *Drosophila*. *PLoS Genet* **12**, e1006123  
558           (2016).
- 559 29.       Chen, D. *et al.* Gilgamesh is required for the maintenance of germline stem cells  
560           in *Drosophila* testis. *Sci Rep* **7**, 5737 (2017).
- 561 30.       Yamashita, Y.M., Jones, D.L. & Fuller, M.T. Orientation of asymmetric stem cell  
562           division by the APC tumor suppressor and centrosome. *Science* **301**, 1547-1550  
563           (2003).
- 564 31.       Sheng, X.R. & Matunis, E. Live imaging of the *Drosophila* spermatogonial stem  
565           cell niche reveals novel mechanisms regulating germline stem cell output.  
566           *Development* **138**, 3367-3376 (2011).
- 567 32.       Manoli, D.S., Fan, P., Fraser, E.J. & Shah, N.M. Neural control of sexually  
568           dimorphic behaviors. *Curr Opin Neurobiol* **23**, 330-338 (2013).
- 569 33.       Geppetti, P., Veldhuis, N.A., Lieu, T. & Bunnett, N.W. G Protein-Coupled  
570           Receptors: Dynamic Machines for Signaling Pain and Itch. *Neuron* **88**, 635-649  
571           (2015).
- 572 34.       Lee, D. Global and local missions of cAMP signaling in neural plasticity, learning,  
573           and memory. *Front Pharmacol* **6**, 161 (2015).

- 574 35. McCudden, C.R., Hains, M.D., Kimple, R.J., Siderovski, D.P. & Willard, F.S. G-  
575 protein signaling: back to the future. *Cell Mol Life Sci* **62**, 551-577 (2005).
- 576 36. Oldham, W.M. & Hamm, H.E. Heterotrimeric G protein activation by G-protein-  
577 coupled receptors. *Nat Rev Mol Cell Biol* **9**, 60-71 (2008).
- 578 37. Boto, T., Gomez-Diaz, C. & Alcorta, E. Expression analysis of the 3 G-protein  
579 subunits, G $\alpha$ , G $\beta$ , and G $\gamma$ , in the olfactory receptor organs of adult  
580 *Drosophila melanogaster*. *Chem Senses* **35**, 183-193 (2010).
- 581 38. Deshpande, G., Godishala, A. & Schedl, P. G $\gamma$ 1, a downstream target for  
582 the hmgcr-isoprenoid biosynthetic pathway, is required for releasing the  
583 Hedgehog ligand and directing germ cell migration. *PLoS Genet* **5**, e1000333  
584 (2009).
- 585 39. Moolenaar, W.H. G-protein-coupled receptors, phosphoinositide hydrolysis, and  
586 cell proliferation. *Cell Growth Differ* **2**, 359-364 (1991).
- 587 40. Kulkarni, M.M. *et al.* Evidence of off-target effects associated with long dsRNAs  
588 in *Drosophila melanogaster* cell-based assays. *Nat Methods* **3**, 833-838 (2006).
- 589 41. Moffat, J., Reiling, J.H. & Sabatini, D.M. Off-target effects associated with long  
590 dsRNAs in *Drosophila* RNAi screens. *Trends Pharmacol Sci* **28**, 149-151 (2007).
- 591 42. Perkins, L.A. *et al.* The Transgenic RNAi Project at Harvard Medical School:  
592 Resources and Validation. *Genetics* **201**, 843-852 (2015).
- 593 43. Filizola, M. & Weinstein, H. The study of G-protein coupled receptor  
594 oligomerization with computational modeling and bioinformatics. *FEBS J* **272**,  
595 2926-2938 (2005).

- 596 44. Milligan, G. G protein-coupled receptor dimerisation: molecular basis and  
597 relevance to function. *Biochim Biophys Acta* **1768**, 825-835 (2007).
- 598 45. Terrillon, S. & Bouvier, M. Roles of G-protein-coupled receptor dimerization.  
599 *EMBO Rep* **5**, 30-34 (2004).
- 600 46. Yoshida, M., Oami, E., Wang, M., Ishiura, S. & Suo, S. Nonredundant function of  
601 two highly homologous octopamine receptors in food-deprivation-mediated  
602 signaling in *Caenorhabditis elegans*. *J Neurosci Res* **92**, 671-678 (2014).
- 603 47. Lukasiewicz, S. *et al.* Hetero-dimerization of serotonin 5-HT(2A) and dopamine  
604 D(2) receptors. *Biochim Biophys Acta* **1803**, 1347-1358 (2010).
- 605 48. Herrick-Davis, K. Functional significance of serotonin receptor dimerization. *Exp*  
606 *Brain Res* **230**, 375-386 (2013).
- 607 49. Xie, Z., Lee, S.P., O'Dowd, B.F. & George, S.R. Serotonin 5-HT1B and 5-HT1D  
608 receptors form homodimers when expressed alone and heterodimers when co-  
609 expressed. *FEBS Lett* **456**, 63-67 (1999).
- 610 50. Pellissier, L.P. *et al.* G protein activation by serotonin type 4 receptor dimers:  
611 evidence that turning on two protomers is more efficient. *J Biol Chem* **286**, 9985-  
612 9997 (2011).
- 613 51. Renner, U. *et al.* Heterodimerization of serotonin receptors 5-HT1A and 5-HT7  
614 differentially regulates receptor signalling and trafficking. *J Cell Sci* **125**, 2486-  
615 2499 (2012).
- 616 52. Borroto-Escuela, D.O., Tarakanov, A.O. & Fuxe, K. FGFR1-5-HT1A  
617 Heteroreceptor Complexes: Implications for Understanding and Treating Major  
618 Depression. *Trends Neurosci* **39**, 5-15 (2016).

- 619 53. Moreno, J.L., Holloway, T., Albizu, L., Sealfon, S.C. & Gonzalez-Maeso, J.  
620 Metabotropic glutamate mGlu2 receptor is necessary for the pharmacological  
621 and behavioral effects induced by hallucinogenic 5-HT<sub>2A</sub> receptor agonists.  
622 *Neurosci Lett* **493**, 76-79 (2011).
- 623 54. Saudou, F., Boschert, U., Amlaiky, N., Plassat, J.L. & Hen, R. A family of  
624 *Drosophila* serotonin receptors with distinct intracellular signalling properties and  
625 expression patterns. *EMBO J* **11**, 7-17 (1992).
- 626 55. Cvejic, S., Zhu, Z., Felice, S.J., Berman, Y. & Huang, X.Y. The endogenous  
627 ligand Stunted of the GPCR Methuselah extends lifespan in *Drosophila*. *Nat Cell*  
628 *Biol* **6**, 540-546 (2004).
- 629 56. Maqueira, B., Chatwin, H. & Evans, P.D. Identification and characterization of a  
630 novel family of *Drosophila* beta-adrenergic-like octopamine G-protein coupled  
631 receptors. *J Neurochem* **94**, 547-560 (2005).
- 632 57. van der Walt, S., Colbert, C., Varoquaux, G. The NumPy Array: A Structure for  
633 Efficient Numerical Computation. *Computing in Science and Engineering*, 22-30  
634 (2011).
- 635 58. van der Walt, S., Schoenberger, J.L., Nunez-Iglesias, J., Boulogne, F., Warner,  
636 J.D., Yager, N., Gouillart, E., Yu, T., and the scikit-image contributors scikit-  
637 image: Image processing in Python. *PerJ:e453* (2014).
- 638 59. Travis, E., Oliphant, E. A guide to NumPy. (2006).
- 639 60. Hunter, J.D. Matplotlib: A 2D Graphics Environment. *Computing in Science and*  
640 *Engineering*, 90-95 (2007). <https://archive.org/details/NumPyBook>.

641 61. Jones, E., Oliphant, E., Peterson, P., *et al* SciPy: Open Source Scientific Tools  
642 for Python. (2001-). <https://www.scipy.org>.

643

644

## 645 **Acknowledgements**

646 The authors dedicate this manuscript to Bruce Baker, who was one of the foremost  
647 scientists in the field, and a great colleague and friend. The authors are grateful to  
648 Richard Zoller, Yue Qian, Megan Aarnio, Heather Kudyba, Jacqueline Uribe,  
649 Chidemman Ihenacho, Stefani Moore, Sampreet Reddy, Amanda Cameron, Chederli  
650 Belongilot, Dylan Ricke, Kenneth Burgess, Amanda Redding, Erin Guillebeau, Jennifer  
651 Murphy, Chantel McCarty, Sarah Murphy, Haley Grable, Mitch Hanson, Haein Kim, and  
652 Sarah Rupert for technical assistance. We thank Bruce Baker, Carmen Robinett,  
653 Edward Kravitz, Matthew Freeman, Mark Brown, Erika Matunis, Steve DiNardo,  
654 Margaret Fuller, Alan Spradling, Hannele Rahuola-Baker, Eric Bohman, Celeste Berg,  
655 Wolfgang Lukowitz, Patricia Moore, Jim Lauderdale, Michael Tiemeyr, Scott Dougan,  
656 Rachel Roberts-Galbraith, and Rhonda Snook for helpful discussions, and Heath Aston  
657 Zachary Letts for comments on the manuscript. We are especially grateful to Barry  
658 Ganetzky for the  $X^{\square}X$ , *shi<sup>ts</sup>* fly stock and to Wolfgang Lukowitz for the use of his  
659 microscope. This work was supported by NSF grants #0841419 and #1355009, and  
660 UGA bridge funds given to CS.

661

## 662 **Author contributions**

663 M.M, B.B.P, and C.S developed and supervised the project, L.F.M coordinated the  
664 mating experiments, K.K. identified the GPCRs expressed in testes tips and developed

665 the computer analysis for the sperm counts, all authors performed the experiments,  
666 M.M, K.K., and CS wrote the manuscript.

667

## 668 **Competing interests**

669 The authors declare no competing interests.

670

## 671 **Tables**

672

### 673 **Table 1. MI<sup>GSC</sup> from control, RNA-*i* and overexpression lines directed against G-** 674 **protein subunits and other signal transducers**

675 UAS-driven expression for the listed genes in the germline via *NG4-1*. BL #:

676 Bloomington stock number, Single and Mated: number of pHH3-positive GSCs/total

677 number of GSCs = MI<sup>GSC</sup>, Diff: MI<sup>GSC</sup> of mated males minus MI<sup>GSC</sup> of non-mated males.

678 For RNA-*i*-lines marked by asterisks siblings outcrossed to *wt* did not show a strong

679 response to mating either, suggesting leakiness of the lines.

680

Genotype	BL#	Crossed to:	MI <sup>GSC</sup> Single	MI <sup>GSC</sup> Mated	Diff.
<i>UAS-G<sub>α</sub>f-i</i>	43201	NG4-1	19/448=4.2%	52/452=11.5%	7.3
	25930*	NG4-1	54/1031=5.2%	76/1183=6.1%	0.9
<i>UAS-G<sub>α</sub>i-i</i>	34924	NG4-1	22/335=6.6%	49/322=15.2%	8.6
	40890	NG4-1	33/597=5.5%	59/536=11%	5.5
	31133	NG4-1	5/269=1.9%	19/285=6.7%	4.8
<i>UAS-G<sub>α</sub>o-i</i>	34653*	NG4-1	23/313=7.3%	26/295=8.8%	1.5
	28010	NG4-1	18/240=7.5%	27/231=11.7%	4.2

<i>UAS-G<sub>α</sub>q-i</i>	36820	NG4-1	24/403=6.0%	32/268=11.9%	5.9
	33765	NG4-1	33/320=10%	50/298=16.8%	6.8
	36775	NG4-1	9/153=5.9%	21/255=8.6%	2.7
	31268	OR	17/233=7.3	15/169=8.9	1.6
		OR	14/335=4.2	12/164=7.3	3.1
		OR	31/568=5.5	27/333=8.1	2.6
		NG4-1	25/556=4.5	8/296=2.7	-2.8
		NG4-1	23/332=6.9	23/291=7.9	1
		NG4-1	23/542=4.2	19/577=3.3	-0.9
		NG4-1	71/1430=5.0	50/1164=4.3	-0.7
	30735	NG4-1	14/318=4.4%	23/293=7.8%	3.4
<i>UAS-G<sub>α</sub>s-i</i>	29576	NG4-1	49/605=8.1%	60/615=9.7%	1.6
	50704	NG4-1	82/1137=7.3%	121/1527=7.9%	0.6
<i>UAS-G<sub>β</sub>5-i</i>	28310	NG4-1	10/306=3.3%	20/292=6.9%	3.6
<i>UAS-G<sub>β</sub>13F-i</i>	35041	NG4-1	38/752=4.8%	46/785=5.7%	0.9
	31134	NG4-1	12/198=6%	31/221=14%	8.0
<i>UAS-G<sub>β</sub>76C-i</i>	28507	NG4-1	14/219=6.4%	26/226=11.5%	5.1
<i>UAS-G<sub>γ</sub>1-i</i>	25934	NG4-1	21/283=7.4%	45/311=14.4%	7.0
	34372	NG4-1	21/434=4.8%	46/400=11.5%	6.7
<i>UAS-G<sub>γ</sub>30A-i</i>	25932	NG4-1	16/319=5.0%	18/286=6.3%	1.3
	34484	NG4-1	9/320=2.8%	31/323=9.6%	6.8
<i>UAS-CaMKI-i</i>	41900	NG4-1	17/337=5.0%	31/328=9.4%	4.4
	35362	NG4-1	10/222=4.5%	17/212=8.0%	3.5
	26726	NG4-1	16/301=5.3%	22/282=7.8%	2.5
<i>UAS-CaMKII-i</i>	35330	NG4-1	49/784=6.2%	91/858=10.6%	4.4
	29401	NG4-1	38/332=11.4%	43/342=12.6%	1.2
<i>UAS-CrebA-i</i>	42526	NG4-1	13/301=4.3%	29/298=9.7%	5.4



<i>UAS-Gprk1-i</i>	35246	NG4-1	13/323=4.0%	15/207=7.4%	3.4
	28354	NG4-1	13/304=4.3%	24/289=12%	7.7
<i>UAS-Gprk2-i</i>	41933	NG4-1	3/218=1.4%	24/228=10.5%	9.1
	35326	NG4-1	12/268=4.5%	35/267=13.1%	8.6
<i>UAS-IP3K-i</i>	35296	NG4-1	10/225=4.4%	14/152=9.2%	4.8
	31733	OR	25/336=7.4%	31/331=9.4%	2.0
	31733	NG4-1	67/572=11.7%	57/555=10.3%	-1.4
<i>UAS-PKC53E-i</i>	34716	NG4-1	18/304=5.9%	22/289=7.6%	1.7
<i>UAS-PKC98E-i</i>	29311	NG4-1	14/293=4.8%	15/284=5.3%	0.5
	35275	OR	9/266=3.4%	25/288=8.4%	5.0
		NG4-1	49/657=7.5%	45/603=7.5%	0.0
	44074	OR	30/597=5.1	36/346=10.4	5.3
		NG4-1	31/289=10.7	38/318=11.9	1.2
<i>UAS-PLC2-i</i>	33719	NG4-1	23/264=8.7%	37/311=11.9%	3.2
<i>UAS-bsk-i</i>	53310	NG4-1	21/380=5.5%	32/346=9.3%	3.8
<i>UAS-Ira-i</i>	31595	NG4-1	6/272=2.2%	8/190=4.2%	2.0
<i>UAS-kay-i</i>	27722	NG4-1	11/256=4.3%	25/259=9.6%	5.3
	31322	NG4-1	22/384=5.7%	61/334=18.3%	12.6
	31391	NG4-1	24/291=8.2%	29/218=13.3%	5.1
<i>UAS-rl-i</i>	36059	NG4-1	21/269=7.8%	32/297=10.8%	3.0
<i>UAS-wt-5-HT1A</i>	27630	NG4-1	16/335=4.8%	30/302=10%	5.2
	27631	NG4-1	10/240=4.2%	24/271=8.9%	4.7
<i>UAS-wt-CrebB17A</i>	7220	NG4-1	51/636=8.0%	98/628=15.6%	7.6
	9232	NG4-1	32/637=5.0%	84/592=14.2%	9.2
<i>UAS-wt-CaMK2R3</i>	29662	NG4-1	20/292=6.8%	28/289=10.0%	3.2
<i>UAS- CaMKII. T287A/</i>	29663	NG4-1	16/287=5.6%	25/283=8.8%	3.2
<i>UAS-wt-Gas</i>	6489	NG4-1	32/289=11.1%	39/300=13.0%	1.9

	6489	NG4-1	40/610=6.6%	54/652=8.3%	1.7
<i>UAS-wt-Ira</i>	7216	NG4-1	15/342=4.4%	44/378=11.6%	7.2
<i>UAS-wt-Kay</i>	7213	NG4-1	24/341=7.4%	70/350=20.0%	12.6

681

682

683

684 **Table 2. MI<sup>GSC</sup> from select RNA-*i*-lines directed against GPCRs**

685 UAS-driven expression of RNA-*i* for the listed GPCRs *i* via *NG4-1* did not block the  
 686 increase in MI<sup>GSC</sup> in response to mating. BL #: Bloomington stock number, Single and  
 687 Mated: number of pHH3-positive GSCs/total number of GSCs = MI<sup>GSC</sup>, Diff: MI<sup>GSC</sup> of  
 688 mated males minus MI<sup>GSC</sup> of non-mated males. Note the variability in MI<sup>GSC</sup> among the  
 689 different genotypes. GPCRs marked by asterisks were excluded from further studies  
 690 because their siblings outcrossed to *wt* did not show a stronger response to mating than  
 691 the experimental (GPCR-*i*/*NG4-1*) flies.

692

GPCR	BL #	Single	Mated	Diff.
<i>UAS-5-HT2A-i</i>	31882	25/490=5.1	36/465=7.3	2.2
	56870	19/582=3.3	32/553=5.8	2.5
<i>UAS-5-HT2B-i</i>	60488	6/261=2.3	21/272=7.7	5.4
	25874	4/228=1.7	34/236=14.4	12.7
<i>UAS-Ado-R-i</i>	27536	11/276=4.0	20/209=9.6	5.6
<i>UAS-AKHR-i</i>	29577	23/492=4.7	54/574=9.4	4.7
<i>UAS-AR-2-i</i>	25935	13/363=3.6	25/336=7.4	3.6
<i>UAS-CG13229-i</i>	29519	9/285=3.2	33/297= 11.1	7.9
<i>UAS-CG14539-i</i>	25855	21/318=6.6	31/307=10.1	3.5

<i>UAS-CG15556-i</i>	44574	28/425=6.6	43/401=10.7	4.1
<i>UAS-CG15744-i</i>	28516	18/279=6.4	27/252=10.7	4.3
	42497	23/323=7.1	36/236=11.0	3.9
<i>UAS-CG30106-i</i>	27669	10/244=4.1	34/273=12.4	8.3
<i>UAS-CG33639-i</i>	28614	32/300=10.7	47/371=12.7	2.0
<i>UAS-CCHaR1-i*</i>	51168	27/407=6.6	27/323=8.4	1.8
<i>UAS-Cry-i</i>	43217	43/389=11.0	75/521=14.4	3.4
<i>UAS-CrzR-i</i>	52751	14/337=4.2	31/333=9.3	5.1
<i>UAS-Dop1R1-i</i>	62193	12/352=3.4	25/308=8.1	4.6
	55239	11/300=3.7	44/267=16.5	12.8
<i>UAS-GABA</i> <i>BR2-i</i>	50608	6/176=3.4	35/207=16.9	13.5
	27699	7/291=2.4	18/282=6.4	4.0
<i>UAS-GABA</i> <i>BR3-i</i>	42725	10/190=5.3	28/243=11.5	6.2
<i>UAS-Moody-i</i>	36821	5/301=1.7	16/234=6.8	5.1
<i>UAS-Mth-I1-i</i>	41930	11/279=4.0	42/300=14.0	10
<i>UAS-Mth-I3-i</i>	41877	54/817=6.6	81/850=11.8	5.2
	36822	19/231=8.2	39/241=16.2	8.0
<i>UAS-Mth-I8-i</i>	36886	48/933=5.1	70/915 =7.6	2.5
<i>UAS-Mth-I9-i</i>	51695	61/985=6.2	82/910 =9.0	2.8
<i>UAS-Mth-I15-i</i>	28017	14/349=4.0	25/337=7.1	3.1
<i>UAS-PK1R-i</i>	27539	28/478=5.9	37/375=9.9	4.0
<i>UAS-Smo-i</i>	27037	12/263=4.6	33/288=11.4	6.8
	43134	19/274=7.0	15/147=10.2	3.2
<i>UAS-Tre1-i</i>	34956	5/234=2.1	28/252=11.1	9.0
<i>UAS-TKR86D-i*</i>	31884	31/564=5.5	28/394=7.1	1.6

<i>UAS-TKR99D-i</i>	55732	30/506=5.9	49/467=10.5	4.6
	27513	4/240=1.7	30/294=10.2	8.5

693

694 **Table 3. MI<sup>GSC</sup> from additional RNA*i*-lines with modified expression of the GPCRs**  
 695 **blocking the increase in MI<sup>GSC</sup> in mated males**

696 BL #: Bloomington stock number, Single and Mated: number of pHH3-positive

697 GSCs/total number of GSCs = MI<sup>GSC</sup>, Diff: MI<sup>GSC</sup> of mated males minus MI<sup>GSC</sup> of non-

698 mated males.

GPCR	BL #	Single	Mated	Diff.
<i>5HT-1A-i/NG4-1</i>	25834	64/841=7.6	67/777=8.6	1
<i>5HT-1B-i/NG4-1</i>	25833	16/256=6.2	26/268=9.7	3.5
	27635	3/304=1.0	27/317=8.5	7.5
	51842	20/381=5.2	32/375=8.5	3.3
	54006	13/405=3.2	23/351=6.5	3.3
<i>5HT-7-i/NG4-1</i>	32471	8/238=3.4	17/229=7.4	4.0
<i>CG12290-i/NG4-1</i>	42520	4/260=1.5	31/246=12.6	11.1
<i>Mth-i/NG4-1</i>	27495	14/352=4	15/336=4.5	0.5

699

700

701 **Figure legends**

702

703 **Figure 1. Mating increased male stem cell division frequency.**

704 A) Cartoon depicting the stages of *Drosophila* spermatogenesis. Note that every GSC

705 division produces exactly 64 spermatids. GB: gonialblast, SG: spermatogonia, SC:

706 spermatocytes, SP: spermatids.

707 A') The apical tip of a *wt* testis. The FasIII-positive hub (asterix) is surrounded by seven  
708 Vasa-positive GSCs (green), one of which is in mitosis based on anti-pHH3-staining  
709 (arrowhead). Scale bar: 10 $\mu$ m.

710 B-F) Blue: non-mated condition, red: mated condition, \*\*\*: P-value < 0.001, numbers of  
711 GSCs and number of gonads (n=) as indicated.

712 B) Box plots showing the range of MI<sup>GSC</sup>. Lines within boxes represent medians,  
713 whiskers represent outliers.

714 C, D) FDGs showing bin of MI<sup>GSC</sup> (bin width=10) across a population of c) *OR* and D)  
715 *CS* males on the X-axis and the percentage of testes with each MI<sup>GSC</sup> on the Y-axis.

716 E) Bar graph showing SI<sup>GSC</sup> of *OR* males from three independent experiments.

717 F) Graph showing the percentage of EdU-marked *OR* GSCs on the Y-axis and hours of  
718 feeding and mating on the X-axis.

719

## 720 **Figure 2. Mating reduced the mature sperm pool.**

721 A-C) Class 1,2 and 3 seminal vesicles from Mst35B-GFP males. Scale bars: 0.1 mm;  
722 arrows point to GFP-negative regions.

723 D-G) Numbers of seminal vesicles (n=) as indicated, n-m: non-mated, m: mated, \*\*\*: P-  
724 value < 0.001.

725 D-F) Bar graphs showing the distribution of Class 1 to 3 seminal vesicles in non-mated  
726 and mated males at days one to three of the mating experiment. Three fly lines that  
727 carry GFP-marked sperm were used: one that carries Dj-GFP (BL#5417), one that  
728 carries the Mst35B-GFP (BL#58408), and one line that carries both constructs  
729 (BL#58406).

730 G) Box plot showing sperm head volume (based on MST35B-GFP) per seminal vesicle  
731 in non-mated and mated males on days one to three of the experiment.

732

733 **Figure 3. Mating did not affect GSC numbers.**

734 A-E) Blue: non-mated condition, red: mated condition, numbers of gonads (n=) as  
735 indicated, genotypes as indicated.

736 A-E) FDGs showing numbers of GSCs on the X-axis and percentage of testes with the  
737 number of GSCs on the Y-axis. No difference in GSC numbers was observed between  
738 non-mated and mated males from different genetic backgrounds.

739

740 **Figure 4. G-proteins were required for the increase in MI<sup>GSC</sup> in response to**  
741 **mating.**

742 A) Cartoon depicting the activation of G-proteins upon GPCR stimulation by ligand. 1:  
743 G-protein association before GPCR stimulation, 2: G-protein distribution after GPCR  
744 stimulation, 3a-c: downstream signaling cascades. AC: Adenylyl Cyclase, cAMP: cyclic  
745 Adenosine Monophosphate, PKA: Protein Kinase A, CREB: cAMP responsive element-  
746 binding protein, PLC: Phospho Lipase C, DAG: Diacylglycerol, PKC: Protein Kinase C,  
747 MAPK: Map Kinase, IP3: Inositol Triphosphate, CaMK: Calcium<sup>2+</sup>/calmodulin-dependent  
748 protein kinase.

749 B, C) Bar graphs showing MI<sup>GSC</sup>. Blue: non-mated condition, red: mated condition, \*\*\*:  
750 P-value < 0.001, numbers of GSCs as indicated, genotypes as indicated.

751 B) Control animals increased MI<sup>GSC</sup> in response to mating.

752 C) Males expressing *G<sub>αi-i</sub>* or dnG<sub>v</sub>1 in the germline did not increase MI<sup>GSC</sup> after mating.

753

754 **Figure 5. Expression of RNA-*i* against seven distinct GPCRs blocked the increase**

755 **in MI<sup>GSC</sup> in response to mating.**

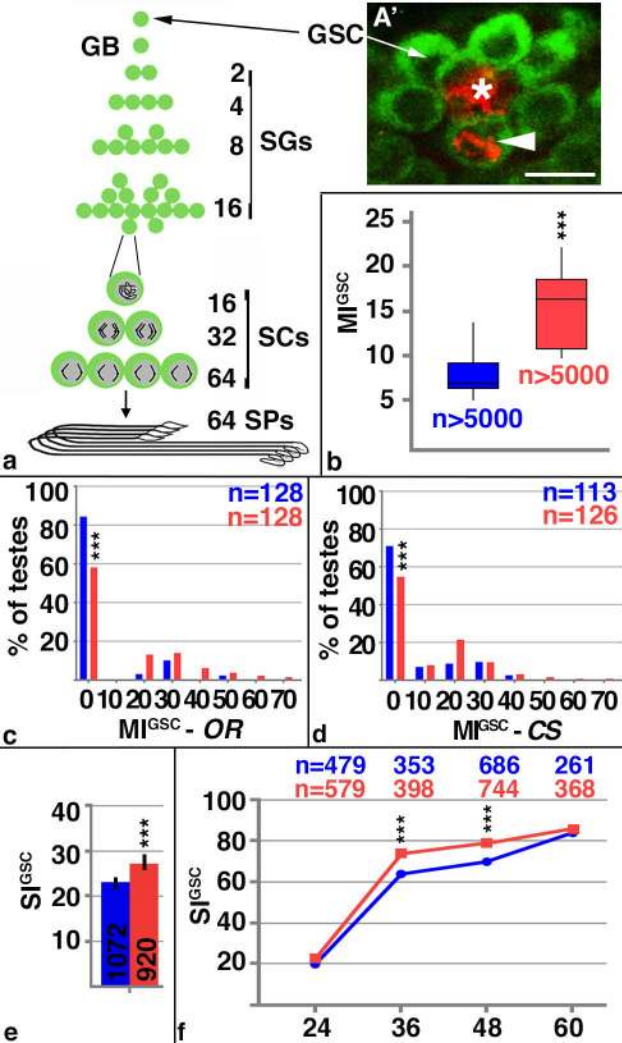
756 A-C) Bar graphs showing MI<sup>GSC</sup>. Blue: non-mated condition, red: mated condition, \*\*\*:

757 P-value < 0.001, numbers of GSCs as indicated, genotypes as indicated.

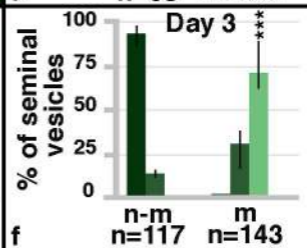
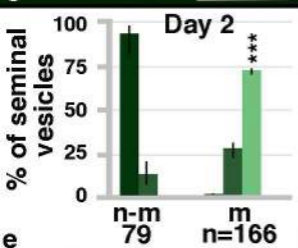
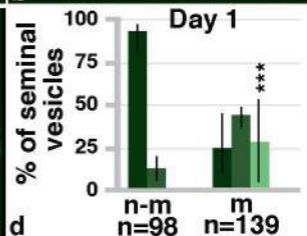
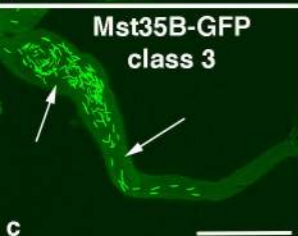
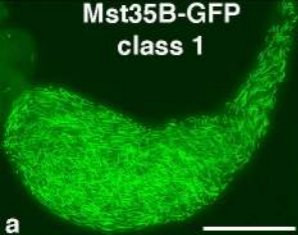
758 A) Control males have significantly higher MI<sup>GSC</sup> than their non-mated siblings.

759 B, C) Mated (B) *GPCR-i*/NG4-1 and (C) *GPCR-i*/NG4-2 males did not have significantly

760 higher MI<sup>GSC</sup> compared to their non-mated siblings.







■ class 1    ■ class 2    ■ class 3

